571535

Sandia National Laboratories

Operated for the United States Department of Energy
by National Technology and Engineering Solutions
of Sandia, LLC.

Albuquerque, New Mexico 87185-0101
Livermore, California 94551-0969

date: June 10, 2019

to: SNL WIPP Records Center
Defense Waste Management Programs

from: Paul S. Domski, MS 1395 (Org. 08882) Shelly R. Nelson for

subject: Technical Aspects of the Baseline Solubility Model for the CRA-2019 PA

Introduction

This memorandum documents the technical evolution of the actinide baseline solubility model from the CRA-2014 PA (Brush and Domski, 2013) model to the CRA-2019 PA (Domski and Sisk-Scott, 2019) model. This memorandum investigates and explains the output chemistry of the CRA-2019 PA baseline solubility model, and how changes to the model since CRA-2014 PA have impacted the results.

The changes to the model for CRA-2019 PA include an updated Pitzer-thermodynamic EQ3/6, version 8.0a, (Wolery and Jarek, 2003) database, DATA0.FM4, (Domski, 2019) which includes various updates, and additions, to solid and aqueous species log K values, and the addition of two new chemical systems for iron and lead. Implementation the new database allowed for the inclusion of new reactant phases in the model to represent the lead shielding used in the waste containers, and the iron components of the waste and waste canisters. Inclusion of these two new chemical systems in the model is a significant change to the solubility model and required that multiple preliminary model runs be executed to test if model assumptions in place for CRA-2014 PA where still valid with this new model. Indeed, it was found that a previous model assumption, the suppression of calcite, was no longer valid, and that calcite would be allowed to form in the CRA-2019 PA baseline solubility model.

Note, all files for this technical memorandum can be found at:
/nfs/data/CVSLIB/WIPP_EXTERNAL/ap153_solubility tech memo

Method

To systematically test and compare the various model inputs and their impact on the results a matrix of runs was executed. All runs use the standard WIPP brines, GWB and ERDA-6, at the highest organic ligand concentration, hereafter, the 1x volume case. First a series of runs tested how the updated database, DATA0.FM4, compared with the previous database, DATA0.FM1, used for CRA-2014 PA. Secondly, a series of runs were performed which tested how the additions of the lead and iron systems effected the results, and finally the assumption of calcite formation is tested. The run matrix is shown in Table 1.

Table 1. Run matrix to test the new aspects of the baseline solubility model for 2019.

	Tests Database				Tests Reactants			Tests Calcite Assumption		Tests Carbonate Phase
Matrix Column	1[A]	2	3	4	5	6	7	8	9[A]	10
Organic/Reactant Budget	CRA-2014	CRA-2014	CRA-2019	CRA-2019	CRA-2019	CRA-2019	CRA-2019	CRA-2019	CRA-2019	CRA-2019
Database	DATA0.FM1	DATA0.FM4	DATA0.FM1	DATA0.FM4	DATA0.FM4	DATA0.FM4	DATA0.FM4	DATA0.FM4	DATA0.FM4	DATA0.SSL
Reactants[B]	default	default	default	default	+lead	+iron	+lead & iron	default	+lead & iron	+lead & iron
Calcite	suppressed	suppressed	suppressed	suppressed	suppressed	suppressed	suppressed	precipitate	precipitate	precipitate

A – Column 1 is the CRA-2014 PA, Column 9 is the CRA-2019 PA.
B – The default reactants are halite, anhydrite, brucite, and hydromagnesite5424.

Comparison of DATA0.FM1 to DATA0.FM4

For convenience DATA0.FM1 will be called "FM1", and DATA0.FM4 will be called "FM4" for the remainder of the memo. To test the effect of the database on the model results four runs were executed for each brine type, GWB and ERDA-6, at the 1x volume case. The first two runs used the CRA-2014 PA organics budget each run with FM1 and FM4, and a second set runs with the CRA-2019 PA organics budget without the lead and iron reactants, as FM1 does not include these systems.

Tables 2 and 3 provide the run matrix and results of the comparison between the DATA0.FM1 and DATA0.FM4 databases. The 1x volume runs for GWB and ERDA-6 brines were used as the comparitive case. The four runs, columns 1 - 4 in the tables compare how the results are effected by the database, FM1 versus FM4, in runs which differ only by the organic ligand budgets. The first two runs use the ligand budget from CRA-2014 PA of Brush and Domski (2013), and the second two runs use the 2019 budget of Sisk-Scott (2019). The reactant phases, halite, anhydrite, brucite, and hydromagnesite(5424) are all present in excess (see Table 4 in Domski and Sisk-Scott, 2019), in other words the reactions reach equilibrium before any of the reactants are exhausted. The discussion that follows will focus on how the database influences the outputs.

Table 2. GWB Outputs for the 1x volume case.

	Column 1	**Column 2**	**Column 3**	**Column 4**
Organic Budget	CRA-2014 PA	CRA-2014 PA	CRA-2019 PA	CRA-2019 PA
Database	DATA0.FM1	DATA0.FM4	DATA0.FM1	DATA0.FM4
Calcite	suppressed	suppressed	suppressed	suppressed
Reactants	halite, anhydrite, brucite, and hydromagnesite(5424)			
File Name	gwb2014.6o	gw14fm4.6o	gw19fm1.6o	gw19fm4.6o
B	0.186	0.186	0.186	0.186
Na	4.77	4.77	4.76	4.76
Mg	0.330	0.330	0.334	0.333
K	0.550	0.550	0.550	0.550
Ca	1.11E-02	1.11E-02	1.11E-02	1.11E-02
Fe	-	-	-	-
S	0.216	0.217	0.216	0.216
Cl	5.36	5.36	5.36	5.36

	Column 1	Column 2	Column 3	Column 4
Br	3.13E-02	3.13E-02	3.13E-02	3.13E-02
Pb	-	-	-	-
Th(IV)	6.05E-08	5.52E-08	6.05E-08	5.52E-08
Np(V)	2.77E-07	3.86E-07	3.04E-07	4.27E-07
Am(III)	2.59E-06	1.62E-07	2.74E-06	1.62E-07
fCO_2	3.14E-06	2.02E-06	3.14E-06	2.02E-06
IS(M)	6.44	6.44	6.43	6.44
pH[A]	8.82	8.82	8.82	8.82
pcH	9.54	9.54	9.54	9.54
Mass of solvent water (kg)	0.737	0.737	0.737	0.737
a(w)	0.735	0.735	0.735	0.735
TIC(M)	3.79E-04	2.44E-04	3.79E-04	2.44E-04

A - Pitzer pH

Table 3. ERDA-6 Outputs for the 1x volume case.

	Column 1	Column 2	Column 3	Column 4
Organic Budget	CRA-2014 PA	CRA-2014 PA	CRA-2019 PA	CRA-2019 PA
Database	DATA0.FM1	DATA0.FM4	DATA0.FM1	DATA0.FM4
Calcite	suppressed	suppressed	suppressed	suppressed
Reactants[A]	halite, anhydrite, brucite, and hydromagnesite(5424)			
File Name	erda_2014.6o	er14fm4.6o	er19fm1.6o	er19fm4.6o
B	6.2 E-02	6.2 E-02	6.2 E-02	6.2 E-02
Na	5.30	5.31	5.30	5.30
Mg	0.136	0.132	0.134	0.134
K	0.096	0.096	0.096	0.096
Ca	1.16E-02	1.18 E-02	1.19 E-02	1.19 E-02
Fe	-	-	-	-
S	0.182	0.180	0.179	0.179
Cl	5.24	5.24	5.23	5.23
Br	1.09E-02	1.09E-02	1.09E-02	1.09E-02
Pb	-	-	-	-
Th(IV)	7.02E-08	6.24E-08	7.06E-08	6.24E-08
Np(V)	8.76E-07	1.18E-06	9.72E-07	1.28E-06
Am(III)	1.48E-06	9.53E-08	1.76E-06	9.54E-08
fCO2	3.14E-06	2.02E-06	3.14E-06	2.02E-06
IS(M)	5.98	5.97	5.97	5.97
pH[B]	8.99	9.00	9.00	9.00
pcH	9.69	9.70	9.70	9.70
Mass of solvent water (kg)	0.888	0.888	0.888	0.888

	Column 1	Column 2	Column 3	Column 4
a(w)	0.747	0.747	0.747	0.747
TIC(M)	4.54E-04	2.96E-04	4.59E-04	2.96E-04

A - All runs include halite, anhydrite, brucite, and hydromagnesite(5424)
B - Pitzer pH

Examination of columns 1 – 4 in Tables 2 and 3 reveals that the bulk solution chemistry calculated by DATA0.FM1 is nearly identical to that calculated using DATA0.FM4. The pH and ionic strength values are identical, as are the concentrations of major elements identical for both databases. However, there are some subtle differences in the actinide concentrations, particularly regarding Am(III) which is a factor of 16 to 17 less as calculated with DATA0.FM4 versus the DATA0.FM1 values. The reason for the drop in Am(III) solubility calculated with DATA0.FM4 are the updated values of the $MgEDTA^{2-}$ and $CaEDTA^{2-}$ log K values used in DATA0.FM4 which increased the stability of these aqueous species relative to the values included in DATA0.FM1. This increased stability of the alkaline earth element complexes with EDTA results in less EDTA being available to complex with Am(III), and thus the decreased solubility of Am(III).

The Th(IV) concentration decreases slightly for the FM4 runs, this can be attributed to the change in the log K of hydromagnesite(5424) which decreases the total inorganic carbonate (TIC) of the system resulting in lower concentrations of thorium – carbonate aqueous species, thus decreasing the Th(IV) solubility.

The slight increase in total Np(V) observed for the FM4 database runs does not lend itself to a straightforward explanation. It is possibly due to secondary effects of the changes in the Mg, Ca, EDTA, and citrate species Log K values in FM4 which could slightly alter the Np(V) speciation thereby increasing its solubility.

Overall it can be stated that the results obtained using the FM4 database were minimally different than the FM1 database. The greatest difference was the Am(III) concentration which was decreased by using FM4 relative to FM1.

The Effect of Lead and Iron on the Simulated Chemistry

Here we examine how the reactants of lead and iron impact the chemistry and actinide solubilities for the two starting solutions, GWB and ERDA-6 for the 1x volume case. Tables 4 and 5 show the run matrix and the results for GWB and ERDA-6, respectively. The FM4 database was used, and calcite was suppressed for all runs, all runs included halite, anhydrite, brucite, and hydromagnesite(5424) as reactants. Only the presence of the lead reactant, litharge, and/or the iron reactant, $Fe(OH)_2$-Hex was varied. Note that column 1 in both Tables 4 and 5 are the same as column 4 in Tables 2 and 3, this commonality is the link between the effect of the database and the effect of the reactants on the model results.

The results clearly demonstrate that lead has very little impact on the chemistry of the system, as columns 2 and 4 reveal in the two tables, while iron, on the other hand, greatly impacts the solution chemistry. Neither lead nor iron have organic complexes included in DATA0.FM4. The runs which contain iron show an increase in pH, and pcH, of about 0.75 units for GWB and 0.5 units for ERDA-6, increased total inorganic carbon of about an order of magnitude, an increase in solvent water of about 0.5 kg, decrease in conservative element concentrations, and somewhat dramatic changes to the actinide

solubilities. The primary effects of $Fe(OH)_2$-Hex dissolution are the increase in pH, TIC, and mass of solvent water all of which can be explained in terms of the product mineral phases that were precipitating. The secondary effects include the decrease in conservative ion (boron and bromine) concentrations by dilution, decrease in Am(III) concentration because of increased pH, and the increase in Th(IV) via hydroxide and carbonate complexation.

The cause of the increase in pH, TIC, and mass of water can be traced to two mineral dissolution reactions. The first reaction is the dissolution of hydromagnesite(5424) which on a per mole dissolution basis acts to remove six moles of hydrogen ion, adds four moles of bicarbonate, and adds six moles of water to solution, via:

$$Mg_5(CO_3)_4(OH)_2{\bullet}4H_2O + 6H^+ \leftrightarrow 5Mg^{2+} + 4HCO_3^- + 6H_2O$$

The dissolution of ferrous hydroxide ($Fe(OH)_2$-Hex) removes two moles of hydrogen ion, and contributes two moles of water per mole of dissolved ferrous hydroxide, via:

$$Fe(OH)_2(s) + 2H^+ \leftrightarrow Fe^{2+} + 2H_2O$$

Thus, together these two reactions are responsible for the primary changes to the solution chemistry by removing eight moles of hydrogen ion which will cause the pH to increase, while adding eight moles of water and four moles of bicarbonate from the hydromagnesite(5424). These two dissolution reactions are particularly important during a brief interval in the reaction path when other water bearing and H^+ consumptive phases are not yet saturated. It must be noted that in the absence of the ferrous hydroxide reactant these extreme chemical conditions are not observed, the hydromagnesite-brucite buffer reaction dominates the chemistry. A detailed discussion of the reaction path and product mineral phases is included in the following sections.

The additional water added to the system from the above reactions explains the observed dilution of the borate and bromine in the iron runs.

The decrease in the Am(III) concentrations for the runs containing iron is accounted for in the dissolution reaction for the solubility controlling phase for Am(III):

$$Am(OH)_3(s) + 3H^+ \leftrightarrow Am^{3+} + 3H_2O$$

Where three moles of H^+ are required to dissolve one mole of $Am(OH)_3(s)$. Thus, for high-pH conditions the solubility of $Am(OH)_3(s)$ is decreased.

Table 4. Effect of lead and iron reactants on the equilibrium solution composition and solution properties for GWB starting solution.

	Column 1	Column 2	Column 3	Column 4
Organic Budget	CRA-2019 PA	CRA-2019 PA	CRA-2019 PA	CRA-2019 PA
Database	DATA0.FM4	DATA0.FM4	DATA0.FM4	DATA0.FM4
Calcite	suppressed	suppressed	suppressed	suppressed
Lead/Iron[A]	Not included	+lead	+iron	+lead & iron
File Name	gw19fm4.6o	gw19fm4p.6o	gw19fm4f.6o	gwb2019.6o

	Column 1	Column 2	Column 3	Column 4
B	0.186	0.185	0.111	0.111
Na	4.76	4.75	5.38	5.38
Mg	0.333	0.335	0.013	0.013
K	0.550	0.547	0.329	0.329
Ca	0.0111	0.0112	0.0188	0.0188
Fe	-	-	9.08E-06	9.08E-06
S	0.216	0.215	0.142	0.142
Cl	5.36	5.39	5.34	5.34
Br	0.0313	0.0312	0.0188	0.0188
Pb	-	1.83E-02	-	4.14E-04
Th(IV)	5.52E-08	5.50E-08	9.81E-08	9.81E-08
Np(V)	4.27E-07	4.27E-07	1.54E-07	1.54E-07
Am(III)	1.62E-07	1.60E-07	3.05E-08	3.05E-08
fCO2	2.02E-06	2.02E-06	2.02E-06	2.02E-06
IS(M)	6.44	6.43	5.92	5.92
pH[B]	8.82	8.82	9.54	9.54
pcH	9.54	9.54	10.26	10.26
Mass of solvent water (kg)	0.737	0.740	1.24	1.24
a(w)	0.735	0.735	0.745	0.745
TIC(M)	2.44E-04	2.44E-04	1.07E-03	1.07E-03

A - All runs include halite, anhydrite, brucite, and hydromagnesite(5424)
B - Pitzer pH

Table 5. Effect of lead and iron reactants on the equilibrium solution composition and solution properties for ERDA-6 starting solution.

	Column 1	Column 2	Column 3	Column 4
Organic Budget	CRA-2019 PA	CRA-2019 PA	CRA-2019 PA	CRA-2019 PA
Database	DATA0.FM4	DATA0.FM4	DATA0.FM4	DATA0.FM4
Calcite	suppressed	suppressed	suppressed	suppressed
Lead/Iron[A]	Not included	+lead	+iron	+lead & iron
File Name	er19fm4.6o	er19fm4p.6o	er19fm4f.6o	erda2019.6o
B	0.062	0.062	0.043	0.043
Na	5.30	5.31	5.49	5.49
Mg	0.134	0.129	0.011	0.011
K	0.096	0.096	0.066	0.066
Ca	0.0119	0.0120	0.0162	0.0163
Fe	-	-	9.11E-06	9.11E-06
S	0.179	0.179	0.132	0.132
Cl	5.23	5.24	5.27	5.27
Br	0.0109	0.0109	0.0075	0.0075

	Column 1	Column 2	Column 3	Column 4
Pb	-	5.27E-03	-	4.05E-04
Th(IV)	6.24E-08	6.26E-08	9.90E-08	9.90E-08
Np(V)	1.28E-06	1.25E-06	7.72E-07	7.72E-07
Am(III)	9.54E-08	9.28E-08	2.94E-08	2.94E-08
fCO2	2.02E-06	2.02E-06	2.02E-06	2.02E-06
IS(M)	5.97	5.96	5.76	5.76
pH[B]	9.00	9.01	9.54	9.54
pcH	9.70	9.71	10.24	10.24
Mass of solvent water (kg)	0.888	0.888	1.29	1.29
a(w)	0.747	0.747	0.750	0.750
TIC(M)	2.96E-04	2.99E-04	1.09E-03	1.09E-03

A - All runs include halite, anhydrite, brucite, and hydromagnesite(5424)

B - Pitzer pH

The three most abundant Th(IV) aqueous species for the four cases are listed in Tables 6 and 7 for GWB and ERDA-6 respectively. Examination of these tables reveals that for the cases that do not include iron (columns 1 & 2 in both tables) the primary Th(IV) species is $Th(OH)_4(aq)$, and for the iron-bearing cases (columns 3 & 4 in both tables) The Th-carbonate species, $Th(OH)_3(CO_3)^-$, dominates and significantly increases the solubility of Th(IV).

Table 6. Th(IV) species showing the effect of lead and iron reactants on the GWB starting solution.

	Column 1	Column 2	Column 3	Column 4
Organic Budget	CRA-2019 PA	CRA-2019 PA	CRA-2019 PA	CRA-2019 PA
Database	DATA0.FM4	DATA0.FM4	DATA0.FM4	DATA0.FM4
Calcite	suppressed	suppressed	suppressed	suppressed
Lead/Iron[A]	Not included	+lead	+iron	+lead & iron
File Name	gw19fm4.6o	gw19fm4p.6o	gw19fm4f.6o	gwb2019.6o
$Th(OH)_3(CO_3)^-$ (M)	9.70E-09	9.68E-09	5.11E-08	5.11E-08
$Th(OH)_4(aq)$ (M)	4.55E-08	4.53E-08	4.70E-08	4.70E-08
$Th(CO_3)_5^{6-}$ (M)	4.47E-18	4.96E-18	4.98E-16	4.99E-16
Total:	5.52E-08	5.50E-08	9.81E-08	9.81E-08

A - All runs include halite, anhydrite, brucite, and hydromagnesite(5424)

Table 7. Th(IV) species showing the effect of lead and iron reactants on the ERDA-6 starting solution.

	Column 1	Column 2	Column 3	Column 4
Organic Budget	CRA-2019 PA	CRA-2019 PA	CRA-2019 PA	CRA-2019 PA
Database	DATA0.FM4	DATA0.FM4	DATA0.FM4	DATA0.FM4
Calcite	suppressed	suppressed	suppressed	suppressed
Lead/Iron[A]	Not included	+lead	+iron	+lead & iron
File Name	er19fm4.6o	er19fm4p.6o	er19fm4f.6o	erda2019.6o
$Th(OH)_3(CO_3)^-$ (M)	1.49E-08	1.52E-08	5.10E-08	5.10E-08
$Th(OH)_4(aq)$ (M)	4.75E-08	4.75E-08	4.80E-08	4.80E-08
$Th(CO_3)_5^{6-}$ (M)	4.65E-18	4.86E-18	7.97E-16	7.98E-16
Total:	6.24E-08	6.26E-08	9.90E-08	9.90E-08

A - All runs include halite, anhydrite, brucite, and hydromagnesite(5424)

The Calcite Assumption

Brush et al., (2006) made the argument that some form of carbonate phase, either aragonite, a calcite polymorph of slightly lower solubility, or a magnesian calcite would likely form in the WIPP repository environment, rather than calcite. The argument was based on the effects of single and multi- inhibitors, inorganic elements and compounds, and organic ligands expected to present in the WIPP waste and which are known to "decrease the rate of calcite precipitation" (Brush et al., 2006). However, Xiong and Lord (2006) observed first hand calcite precipitation in XRD patterns of their study of carbonation products of MgO in GWB and ERDA-6. Regardless of this it was the recommendation of Larry Brush that calcite, aragonite, dolomite, magnesite, nesquehonite, and hydromagnesite4323 be "suppressed", i.e., not allowed to precipitate, in the baseline solubility model. This assumption has been in place since CRA-2014 PA, when the EQ3/6 code was first used for these calculations, and for PA's before 2014 when the FMT code was used for the baseline solubility calculations.

During the course of running the baseline solubility model for CRA-2019 PA it was observed that with the addition of the iron reactant, $Fe(OH)_2$-Hex, an interval near the end of the reaction path, for both brines, was dominated by high pH, ~9.5 (pcH ~10.25), and high carbonate concentration, ~1E-03 M, as seen in columns 3 and 4 of Tables 4 and 5. Further examination of the EQ6 output files for these runs revealed that calcite was 50 times (50x) supersaturated during this interval of high pH and carbonate concentration, which was a red flag. Calcite is a very common phase in natural waters, and by preventing its formation in the baseline solubility runs we were forcing the solution chemistry into an unrealistic compositional space. Therefore, additional trial runs were executed with the full suite of reactants, i.e., lead and iron, and with calcite "unsuppressed". The results of these trials were later agreed upon to form the final baseline solubility model for CRA-2019 PA. It remains unclear why Larry Brush recommended that calcite be suppressed when he, in Brush et al (2006), stated that some carbonate phase would form and be present in the WIPP environment, and that calcite was observed to form in MgO carbonation experiments in WIPP brines (Xiong and Lord, 2006).

To gain a more complete understanding of how allowing calcite formation influenced the model output it was important to examine the case which did not include lead and iron as reactants. Four runs for

each brine type will be examined, these include two without lead and iron reactants, one each where calcite is suppressed or not, and two additional runs that include lead and iron and again with calcite suppressed and not. Tables 8 and 9 provide the model outputs for GWB and ERDA-6, respectively.

Table 8. Effect of calcite suppression on the equilibrium solution composition and solution properties for GWB starting solution.

	Column 1	Column 2	Column 3	Column 4
Organic Budget	CRA-2019 PA	CRA-2019 PA	CRA-2019 PA	CRA-2019 PA
Database	DATA0.FM4	DATA0.FM4	DATA0.FM4	DATA0.FM4
Calcite	suppressed	Not suppressed	suppressed	Not suppressed
Lead/Iron[A]	Not included	Not included	+lead & iron	+lead & iron
File Name	gw19fm4.6o	gw19f4c.6o	gwb2019.6o	gwb_1x.6o
B	0.186	0.229	0.111	0.224
Na	4.76	4.69	5.38	4.69
Mg	0.333	0.347	0.013	0.348
K	0.550	0.677	0.329	0.663
Ca	0.0111	0.0109	0.0188	0.0109
Fe	-	-	9.08E-06	2.61E-05
S	0.216	0.232	0.142	0.232
Cl	5.36	5.37	5.34	5.40
Br	0.0313	0.0386	0.0188	0.0378
Pb	-	-	4.14E-04	1.90E-02
Th(IV)	5.52E-08	5.46E-08	9.81E-08	5.45E-08
Np(V)	4.27E-07	4.00E-07	1.54E-07	4.02E-07
Am(III)	1.62E-07	1.65E-07	3.05E-08	1.63E-07
fCO2	2.02E-06	2.02E-06	2.02E-06	2.02E-06
IS(M)	6.44	6.54	5.92	6.53
pH[B]	8.82	8.82	9.54	8.82
pcH	9.54	9.54	10.26	9.54
Mass of solvent water (kg)	0.737	0.597	1.24	0.61
a(w)	0.735	0.732	0.745	0.732
TIC(M)	2.44E-04	2.43E-04	1.08E-03	2.50E-04

A - All runs include halite, anhydrite, brucite, and hydromagnesite(5424)

B - Pitzer pH

Table 9. Effect of calcite suppression on the equilibrium solution composition and solution properties for ERDA-6 starting solution.

	Column 1	Column 2	Column 3	Column 4
Organic Budget	CRA-2019 PA	CRA-2019 PA	CRA-2019 PA	CRA-2019 PA
Database	DATA0.FM4	DATA0.FM4	DATA0.FM4	DATA0.FM4
Calcite	suppressed	Not suppressed	suppressed	Not suppressed
Lead/Iron[A]	Not included	Not included	+lead & iron	+lead & iron
File Name	er19fm4.6o	er19f4c.6o	erda2019.6o	erda_1x.6o
B	0.062	0.281	0.043	0.281
Na	5.30	4.66	5.49	4.66
Mg	0.134	0.435	0.011	0.435
K	0.096	0.512	0.066	0.499
Ca	0.0119	0.0127	0.0163	0.0128
Fe	-	-	9.11E-06	2.67E-05
S	0.179	0.224	0.132	0.224
Cl	5.23	5.18	5.27	5.22
Br	0.0109	0.0581	0.0075	0.0566
Pb	-	-	4.05E-04	1.88E-02
Th(IV)	6.24E-08	5.45E-08	9.90E-08	5.44E-08
Np(V)	1.28E-06	1.20E-06	7.72E-07	1.20E-06
Am(III)	9.54E-08	1.81E-07	2.94E-08	1.78E-07
fCO_2	2.02E-06	2.02E-06	2.02E-06	2.02E-06
IS(M)	5.97	6.48	5.76	6.48
pH[B]	9.00	8.82	9.54	8.82
pcH	9.70	9.52	10.24	9.52
Mass of solvent water (kg)	0.888	0.164	1.29	0.168
a(w)	0.747	0.732	0.750	0.732
TIC(M)	2.96E-04	2.44E-04	1.09E-03	2.50E-04

A - All runs include halite, anhydrite, brucite, and hydromagnesite(5424)

B - Pitzer pH

The results shown in Tables 8 and 9 clearly demonstrate that by allowing calcite to precipitate the chemistry of the system was moderated. What is most striking is the similarity of the compositions in columns 1, 2, and 4, especially since neither columns 1 and 2 include lead and iron reactants, while column 4 does include these reactants. This is especially apparent for GWB, while for the ERDA-6 runs in which calcite was allowed to form the major properties (TIC, fCO_2, and the actinide concentrations) are nearly the equal, but the chemistry of individual ions may differ due to the decrease in the solvent mass. The decrease in the mass of solvent water was caused by the precipitation of hydrated mineral phases and is particularly extreme in the case of ERDA-6 and will be discussed in the following section.

In the previous section the effect of elevated pH and TIC concentration on the solubility of Am(III) and Th(IV) was explained for the cases where lead and iron were present and where calcite was suppressed.

Here we observe that with lead and iron were present and calcite allowed to precipitate the solubility of Am(III) and Th(IV) returns to expected ranges.

The important points to take away from this are: 1) The fact that allowing calcite to precipitate did not appreciably change the chemistry for the two runs which did not include lead and iron reactants builds confidence that the baseline solubility models for previous compliance recertifications applications, 2014 and before, were insensitive to calcite suppression. In other words, the baseline solubilities for CRA-2014, and before, would not change appreciably had calcite been allowed to precipitate. The second point to take away is that by allowing calcite to precipitate in the runs containing iron and lead the chemistry of the system was moderated in a range that is realistic, where otherwise the carbonate system would have been out of equilibrium.

The Baseline Solubility Model EQ6 Reaction Paths

During the preparation of the baseline solubility report for CRA-2019 PA (Domski and Sisk-Scott, 2019) many trial model runs were executed to test the aspects of the model which had changed since CRA-2014 PA. The most revealing of these trial runs are documented in this memo, and the final model runs results, which include all the new model aspects, comprise the CRA-2019 PA actinide source term as documented by Domski and Sisk-Scott (2019).

Figures 1 and 2 are plots of the reaction paths for the 1x volume cases GWB and ERDA-6 brines, respectively, that display the solids phases (reactants and products), fugacity of $CO_2(g)$, and the pcH plotted against the EQ6 reaction progress variable, log ξ, which is the cumulative log base 10 of moles reactants. These plots are useful and interesting because they display how reactants and product phases evolve from the initial brine to the final brine composition.

Reading and understanding these reaction-path plots is best facilitated with the knowledge that the chemsitry evolves from left to right, in other words, the solution composition at the left hand Y-axis is equivalent to the unreacted GWB or ERDA-6 brine composition, while the chemistry at the right-hand Y-axis represents the fully equilibrated compositions.

Figure 1. EQ6 reaction path for GWB (1x volume) showing the reactant and product phases.

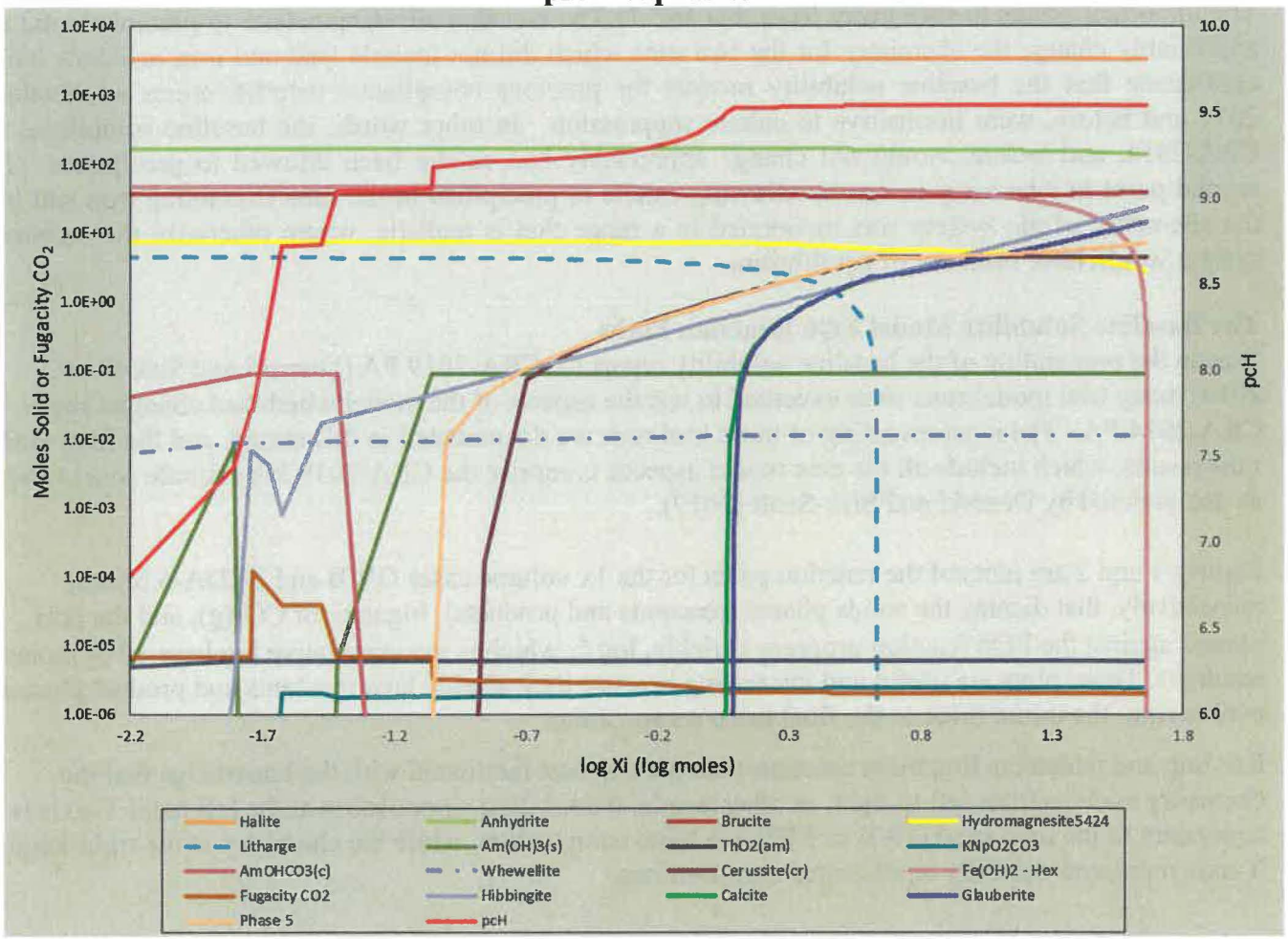

The GWB reaction path for the 1x volume case (Figure 1) shows the importance of the carbonate system in the evolution of the brine chemistry. The early precipitation of the metastable americium phase, $AmOHCO_3(c)$, is caused by the a very high carbonate concentration (16 mM) of the initial solution – the EQ3NR input value. As the reaction progresses $AmOHCO_3(c)$ dissolves and is replaced with $Am(OH)_3(s)$. Hibbingite ($Fe_2Cl(OH)_3$) saturation is reached and continues on a 1:2 mole basis with the dissolution of $Fe(OH)_2$-Hex until this phase is exhausted at the end of the reaction path.

The calcium oxalate phase, whewellite ($CaC_2O_4 \cdot H_2O$), precipitates from solution immediately at the start of the reaction path and remains in the system in equilibrium with the solution until the reaction path terminates. Interestingly, whewellite is the only organic solubility-limiting phase that forms in either brine.

At $\log \xi = -1$ Phase 5 ($Mg_3Cl(OH)_5 \cdot 4H_2O$) reaches saturation and precipitation begins in response to continued hydromagnesite(5424) dissolution. Phase 5 continues to precipitate until the lead reactant, litharge, is expended at which point the rate of Phase 5 accumulation is greatly reduced.

The lead reactant phase, litharge (PbO), dissolves until cerussite ($PbCO_3$) saturation is achieved, and continues to precipitate in a 1:1 mole ratio with the continued dissolution of litharge. Cerussite also acts

as a sink for carbonate liberated from the dissolution of hydromagnesite(5424). Litharge is exhausted at log $\xi = 0.64$ at which point cerussite precipitation ceases, and cerrusite in equilibrium acting as the solubility controling phase for lead for the remainder of the reaction path.

Calcite precipitation commences at log $\xi = 0.067$, followed immediately by Glauberite ($Na_2Ca(SO4)_2$). The precipitation of calcite requires a source of Ca^{2+} which is supplied by dissolving anhydrite which also adds additional sulfate to the system, which in turn facilitates Glauberite precipitation. Note that once calcite precipitation begins the pH of the system plateaus and is constant once all of the litharge as precipitated as cerussite. From this point on (log $\xi = 0.64$) in the reaction path the pH is constant, and it is the equilibrium between calcite, brucite, and hydromagnesite(5424) that sets the equilibrium, or invariant point, and determines the final fCO_2 and TIC of the system.

The GWB reaction path terminated when all of the reactant $Fe(OH)_2$-Hex was exhausted, the reaction path continued to this point because this reactant phase never reached equilibrium with the solution ($SI_{Fe(OH)2\text{-}Hex} < 0$), all of the other phases in the system, both reactants and products, were in equilibrium with the solution.

The pH, or pcH as depicted in Figure 1 shows a steady increasing trend with jumps and plateaus as the reaction path advances. These pH jumps are caused by the appearance of new products, the exhaustion of reactants, or combinations of both. The final pH plateau represents the final invariant conditions of the system as discussed above.

Note that the actinide solubility controlling phases are not included as reactants in the EQ6 runs, rather the concentrations of Am(III), Th(IV), and Np(V) are set to be in equilibrium with their solubility controlling phases in the EQ3NR input files at the starting brine compositions. At the initiation of the EQ6 run the solubility controlling phase for each actinide, except for Am(III) as discussed above, precipitates as these phases are less soluble in the evolving solution than they were in the initial solution. It was not necessary to place constraints on which phase could form, however, the model output was checked to ensure that the preferred phases had formed. All of the actinide solubility-limiting phases were present and maintained their saturation throughout the entire reaction path.

Table 10 provides the solid-phase accounting for both reactants and products for the GWB reaction path. The phases halite, anhydrite, brucite, hydromagnesite(5424), litharge, and $Fe(OH)_2$-Hex were the defined reactants for CRA-2019 PA, their initial values are the same as those listed in Table 4 of Domski and Sisk-Scott (2019). Note that in Table 10 negative values of delta indicate dissolution, and positive values indicate precipitation. With the exception of $AmOHCO_3$(c) and whewellite, all of the product phases have zero initial moles. $AmOHCO_3$(c) and whewellite have non-zero initial moles because they were identified as super saturated by the initial EQ3NR run, therefore, upon initiation of the reaction-path calculations EQ6 first precipitates these phases to equilibrate them with the solution such that their saturation index is zero.

Table 10. Initial and Final Solid Phase Accounting for GWB Starting Solution.

Phase	Initial (mols)	Final (mols)	Delta (mols)
Halite	3486.1	3457.8	-28.30
Anhydrite	166.28	137.94	-28.34
Brucite	36.7	39.1	2.43
Hydromagnesite(5424)	7.34	2.72	-4.62

Phase	Initial (mols)	Final (mols)	Delta (mols)
Litharge	4.35	0.00	-4.35
$Fe(OH)_2$-Hex	46.08	0.00	-46.08
$AmOHCO_3$(c)	0.0115	0.00	-0.01
$Am(OH)_3$(s)	0.00	0.0893	0.0893
ThO_2(am)	0.00	5.85E-06	0.00
$KNpO_2CO_3$	0.00	2.39E-06	0.00
Whewellite	0.00216	0.0111	0.01
Cerussite(cr)	0.00	4.34	4.34
Hibbingite	0.00	23.04	23.04
Calcite	0.00	14.2	14.16
Glauberite	0.00	14.2	14.18
Phase 5	0.00	7.15	7.15

The values in Table 10 provide insight into the mass balance of reactant and product phases. For example, ~28.3 moles of halite and anhydrite dissolved, while ~14.2 moles of calcite and glauberite, each containing 1 mole of calcium, precipitated accounting for all of the calcium from anhydrite dissolution. Glauberite contains two moles of sodium per mole, which accounts for the sodium contributed by halite. This element by element accounting can be done for all of the elements included in these simulations that participate in reactions with solid phases.

Figure 2 provides the ERDA-6 reaction path for the 1x volume case for the CRA-2019 PA baseline solubility. The ERDA-6 reaction path looks similar to the GWB reaction path (Figure 1) with the difference being the "timing" of the appearance of key phases along the reaction path. The two most obvious are calcite and glauberite, each reach saturation earlier in the ERDA-6 reaction path compared to the GWB reaction path. The appearance of Borax, or sodium tetraborate, ($Na_2B_4O_7 \cdot 10H_2O$) late in the ERDA-6 reaction path is unique and caused by the concentration of the borate ion as the amount of solvent water decreased due to the precipitation of Phase 5 and other hydrated phases.

Like GWB, the ERDA-6 reaction path terminated when all of the reactant $Fe(OH)_2$-Hex was exhausted, the reaction path continued to this point because this reactant phase never reached equilibrium with the solution ($SI_{Fe(OH)2\text{-}Hex} < 0$), all of the other phases in the system, both reactants and products, were in equilibrium with the solution.

Figure 2. EQ6 reaction path for ERDA-6 (1x volume) showing the reactant and product phases.

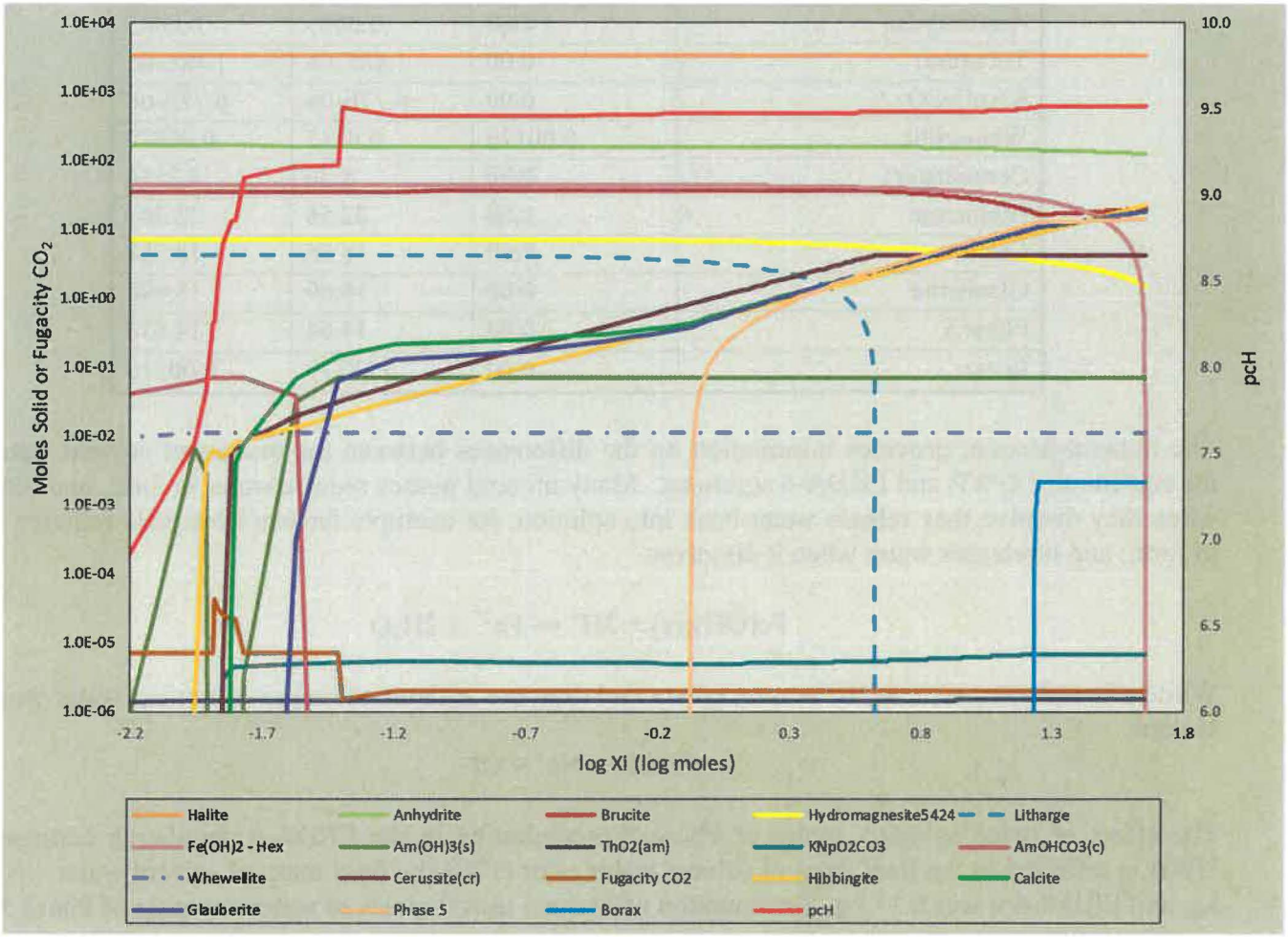

The solid phase accounting for the ERDA-6 reaction path at 1x volume is documented in Table 11. The values in Table 11 are very similar to the GWB values in Table 10 with two notable exceptions: 1) For GWB 2.4 moles of brucite formed, and for ERDA-6 15.5 moles of brucite dissolved; 2) 7.2 moles of Phase 5 formed in GWB, while 14.6 moles formed in ERDA-6. This difference in the magnesium system was caused by the differences in the initial magnesium concentrations in the two brines where ERDA-6 had 1.9E-02 mol/L, and GWB 1.02 mol/L as documented in Table 2 of Domski and Sisk-Scott (2019).

Table 11. Initial and Final Solid Phase Accounting for ERDA-6 Starting Solution.

Phase	Initial (mols)	Final (mols)	Delta (mols)
Halite	3413.8	3380.4	-33.40
Anhydrite	162.84	125.59	-37.25
Brucite	35.94	20.47	-15.48
Hydromagnesite(5424)	7.19	1.49	-5.70
Litharge	4.26	0.00	-4.26
$Fe(OH)_2$-Hex	45.12	0.00	-45.12

Phase	Initial (mols)	Final (mols)	Delta (mols)
$AmOHCO_3(c)$	9.66E-03	0.00	-9.66E-03
$Am(OH)_3(s)$	0.00	0.0685	0.0685
$ThO_2(am)$	0.00	1.48E-06	1.48E-06
$KNpO_2CO_3$	0.00	6.77E-06	6.77E-06
Whewellite	0.00176	0.0112	0.00947
Cerussite(cr)	0.00	4.26	4.2574
Hibbingite	0.00	22.56	22.561
Calcite	0.00	18.56	18.558
Glauberite	0.00	18.69	18.686
Phase 5	0.00	14.64	14.636
Borax	0.00	0.00210	0.00210

The mineral account provides information on the differences between the masses of solvent water for the equilibrated GWB and ERDA-6 solutions. Many mineral phases require water to form, and likewise when they dissolve they release water back into solution, for example ferrous hydroxide requires water to form, and it releases water when it dissolves.

$$Fe(OH)_2(s) + 2H^+ \leftrightarrow Fe^{2+} + 2H_2O$$

While other phases, such as halite, precipitate and dissolve without adding or removing water from the system.

$$NaCl \leftrightarrow Na^+ + Cl^-$$

The effect of twice as many moles of Phase 5 precipitating in the ERDA-6 simulation compared to GWB is reflected in the final mass of solvent water. For GWB the final mass of solvent water was 0.61 kg, and ERDA-6 it was 0.17 kg. Precipitation of Phase 5 uses 9 moles of water per mole of Phase 5, via:

$$3Mg^{2+} + Cl^- + 9H_2O \leftrightarrow Mg_3Cl(OH)_5{\bullet}4H_2O + 5H^+$$

Phase 5 precipitation was the primary cause of the difference in the final masses of the two brine types, however, all phases that include water in their mass-action expressions played a role. A detailed accounting of the change in the moles of water consumed or liberated by mineral phases over the reaction path may be calculated as the sum of the products of "Delta" value(s) as provided in Tables 10 and 11, with the number of moles of the water of formation for each mineral phase. For example, for ERDA-6 for Phase 5:

(9 mols H_2O/mol Phase 5) x (14.64 mols of Phase 5) = 131.72 mols H_2O

The sum of the moles of water that include water in their mass-action expressions provides the total change in moles (mass) of solvent water from the initial to final solution compositions.

Table 12 provides the total, moles and mass, decrease in the mass of solvent water via mineralogic reactions from the initial solution to the final equilibrated solutions.

Table 12. Accounting of water consumed or liberated by mineralogic reactions.

Phase	Mols H_2O/Mol Phase	ERDA-6 (mols H_2O)	GWB (mols H_2O)
Halite	0	0.00	0.00
Anhydrite	0	0.00	0.00
Brucite	2	-30.95	4.85
Hydromagnesite(5424)	6	-34.20	-27.72
Litharge	1	-4.26	-4.35
$Fe(OH)_2$-Hex	2	-90.25	-92.15
$AmOHCO_3(c)$	1	-0.01	-0.01
$Am(OH)_3(s)$	3	0.21	0.27
$ThO_2(am)$	2	0.00	0.00
$KNpO_2CO_3$	0	0.00	0.00
Whewellite	1	0.01	0.01
Cerussite(cr)	0	0.00	0.00
Hibbingite	3	67.68	69.11
Calcite	0	0.00	0.00
Glauberite	0	0.00	0.00
Phase 5	9	131.72	64.36
Borax	1	0.00	0.00
Moles of H_2O Consumed in Rxn Path		39.96	14.36
Mass (kg) of H_2O Consumed in Rxn Path		0.72	0.26

Examination of Table 12 shows that dissolution $Fe(OH)_2$-Hex and hydromagnesite(5424) contributed the greatest amounts of water at ~91 and ~30 moles, respectively. Brucite contributes 31 moles to ERDA-6, while for GWB it removes ~5 moles. Precipitation of Hibbingite removes ~68 moles from both brines, and Phase 5 removes 132 moles from ERDA-6, while only 64 moles for GWB. The cumulative change was 40 moles (0.72 kg) for ERDA-6 and 14 moles (0.26 kg) for GWB. The initial mass of solvent water, as calculated by EQ6 was 0.89 and 0.87 kg for ERDA-6 and GWB, respectively, and their final masses are 0.17 and 0.61 kg, respectively. These final solvent masses confirm the EQ6 output values provided in Tables 8 and 9 Column 4 for ERDA-6 and GWB, respectively.

The ERDA-6 brine is a sodium chloride brine, with very little magnesium, while GWB is a sodium – chloride – magnesium brine, with magnesium contributing about 20% of the equivalent concentration. It is the difference in the initial brine compositions that accounts for the nearly twice as much Phase 5 precipitating in ERDA-6 compared to GWB, and the consequential loss of solvent water in ERDA-6.

Despite the initial differences in the compositions of ERDA-6 and GWB, their equilibrium compositions are remarkably similar. Table 13 provides the equilibrium concentrations for the 1x volume case as reported in Domski and Sisk-Scott (2019) for GWB and ERDA-6.

Table 13. GWB and ERDA-6 equilibrated compositions for the 1x case, all concentrations are in molarity (M) unless otherwise noted.

Element/Property	GWB	ERDA-6
B	0.224	0.281
Na	4.69	4.66
Mg	0.348	0.435
K	0.663	0.499
Ca	0.0109	0.0128
Fe	2.61E-05	2.67E-05
S	0.232	0.224
Cl	5.40	5.22
Br	0.0378	0.0566
Pb	1.90E-02	1.88E-02
Th(IV)	5.45E-08	5.44E-08
Np(V)	4.02E-07	1.20E-06
Am(III)	1.63E-07	1.78E-07
fCO_2	2.02E-06	2.02E-06
Ionic Strength	6.53	6.48
pH[A]	8.82	8.82
pcH	9.54	9.52
Mass of solvent water (kg)	0.610	0.168
a(w)	0.732	0.732
Total Inorganic Carbon	2.50E-04	2.50E-04

A – Pitzer pH

The similarity of the equilibrium compositions of GWB and ERDA-6 can be explained in terms of the rock to water ratio of the modeled system. If we convert the moles of reactants (halite, anhydrite, brucite, hydromagnesite(5424), litharge, and ferrous hydroxide) to mass units we get a total mass of 237 kg for GWB and 232 kg for ERDA-6. Thus, with the 1 kg of working solution in EQ3/6 the mass-based rock to water ratio is 237 for GWB and 232 for ERDA-6. At these very high ratios it should be expected that the equilibrium solution compositions will be dominated by the rock, or reactant composition, even for very different starting solution compositions. This observation brings into question the necessity of using different starting brine compositions.

Mass of Solvent Water: A Look at Other Possibilities

The decrease in the mass of solvent water for ERDA-6 warranted further study. By allowing calcite to precipitate a shift in the product phases of the model occurred which resulted in large quantities of Phase 5 to form and the subsequent depletion of water. Brush et al. (2006) argued that the presence of inhibitors would likely favor the precipitation of a magnesian calcite phase, a phase that is not included in DATA0.FM4. To test if a hybrid magnesian calcite phase was stable in WIPP brines under these conditions, and if so, its effect on the equilibrium chemistry a non-QA'd database was created by copying DATA0.FM4 to "DATA0.SSL" and a solid solution data block was added. Wolery and Jarek (2003) state that the "The solid solutions currently used in EQ3/6 data files are ideal site-mixing models treating mixing over only one site." In other words, the composite solid solution would be comprised of (mole) fractions of the pure end-member phases. Note, this database, DATA0.SSL in non-QA and was created for illustrative purposes only, and it will be included in the records package for this memo.

Based on working assumptions and knowledge of WIPP experimental systems it was decided that the pure end-member phases would be calcite and hydromagnesite(5424). Magnesite was not considered because of kinetic considerations, and hydromagnesite(5424) was chosen because it has been observed to form in WIPP brines (Brush et al., 2006)

The data block that was added to DATA0.SSL is shown below. For the details regarding the data block see Wolery and Jarek (2003).

```
+--------------------------------------------------------------------
solid solutions
+--------------------------------------------------------------------
Calcite-Hydromag          (Ca,Mg)CO3
     sp.type =  ss   ideal

  2 components
     1.0000  Calcite                      1.0000  Hydromagnesite5424
  type  = 1
  0 model parameter(s)
  1 site parameter(s)
  1.000     0.000     0.000     0.000     0.000     0.000
+--------------------------------------------------------------------
```

Having added this solid-solution phase to the database the 1x volume cases for ERDA-6 and GWB were run and the results extracted and tabulated.

Table 14. GWB and ERDA-6 equilibrated compositions for the 1x case using different carbonate phases, all concentrations are in molarity unless otherwise noted.

	GWB		ERDA-6	
Database	DATA0.FM4	DATA0.SSL	DATA0.FM4	DATA0.SSL
Carbonate Phase	Calcite	Calcite-Hydromag	Calcite	Calcite-Hydromag
B	0.224	0.130	0.281	5.05E-02
Na	4.69	4.85	4.66	5.03
Mg	0.348	0.320	0.435	0.294
K	0.663	0.383	0.499	0.078
Ca	1.09E-02	1.05 E-02	1.28 E-02	1.00E-02
Fe	2.61E-05	2.50E-05	2.67E-05	2.43E-05
S	0.232	0.216	0.224	0.198
Cl	5.40	5.36	5.22	5.28
Br	3.78 E-03	2.18 E-03	5.66 E-03	8.81E-03
Pb	1.90E-02	2.47E-02	1.88E-02	2.31E-02
Th(IV)	5.45E-08	5.28E-08	5.44E-08	5.39E-08
Np(V)	4.02E-07	6.70E-07	1.20E-06	3.20E-06
Am(III)	1.63E-07	1.51E-07	1.78E-07	1.41E-07

	GWB		ERDA-6	
fCO_2	2.02E-06	1.43E-06	2.02E-06	1.38E-06
Ionic Strength	6.53	6.34	6.48	6.15
pH[A]	8.82	8.82	8.82	8.82
pcH	9.54	9.53	9.52	9.51
Mass of solvent water (kg)	0.610	1.06	0.168	1.095
a(w)	0.732	0.738	0.732	0.745
Total Inorganic Carbon	2.50E-04	1.79E-04	2.50E-04	1.75E-04

A – Pitzer pH

Comparing the results in Table 14 for GWB and ERDA-6 for the calcite and Calcite-Hydromag runs, using DATA0.SSL, reveals that the equilibrated solution chemistry is nearly identical regardless of which phase was allowed to precipitate. The most obvious difference between the runs is the mass of solvent water, which increased dramatically for the runs with calcite-hydromag. Based on this "back of the envelop" calculation we see that by allowing a mixed Ca – Mg carbonate phase to form in place of pure calcite, the water consumption via Phase 5 precipitation was averted, while the solution chemistry was virtually the unchanged. The possibility of including a mixed Ca – Mg carbonate solid solution in the next QA database requires further study.

Summary and Conclusions

The CRA-2019 PA baseline solubility model (Domski and Sisk-Scott, 2019) includes significant changes compared to the CRA-2014 PA model, and this memorandum was created to document how these changes influenced the model and impacted the final results.

Overall it can be stated that the results obtained using the FM4 database were minimally different than the FM1 database. The greatest difference was the Am(III) concentration which was decreased by using FM4 relative to FM1. The change to the Am(III) concentration was caused by changes to the log K values of the $MgEDTA^{2-}$ and $CaEDTA^{2-}$ aqueous complexes.

The inclusion of the lead and iron inventory items in the model was made possible with the addition of these systems to the DATA0.FM4 database. The lead system had a minimal impact on the solution chemistry. The lead reactant litharge dissolved, and once the cerussite had reached saturation the reaction followed a mole per mole dissolution/precipitation of litharge/cerussite. Note that DATA0.FM4 does not include Pitzer parameters for the lead system, therefore, all activity coefficients for lead aqueous species were calculated via the extended Debye-Huckel expression. Compared to lead, the iron system had a much larger influence on the system chemistry. The primary effects of the dissolution of ferrous hydroxide were increases in solvent water mass, total carbonate concentration, and pH. Secondary effects include dilution of conservative ions, increase in Th(IV) solubility via increased carbonate complexation, and a decrease in Am(III) solubility at high pH.

The increase in equilibrium pH and total inorganic carbon caused by ferrous iron dissolution were flagged as potential concerns, and further examination of model outputs revealed a strong disequilibrium in the carbonate system with calcite supersaturated by 50x. Historically, calcite had been suppressed in the baseline solubility model, but given the circumstances this assumption was reevaluated, and based on Brush et al.'s (2006) discussions this assumption was dismissed and calcite was allowed to form in the EQ6 simulations. By allowing calcite to precipitate the resulting solution compositions were

acceptable with no disparate disequilibrium observed in any of the chemical systems. It was this set of runs for GWB and ERDA-6 that were used in Domski and Sisk-Scott (2019) as the baseline solubility model.

One additional trial was performed using a non-QA database that was created from DATA0.FM4 by adding a solid-solution phase, calcite – hydromagesnite5424. These trials were executed to determine if a mixed calcium – magnesium carbonate phase would be predominant over pure calcite, and if so, would there be any change to the mass of solvent water. The results confirmed that the solid solution phase did precipitate in place of calcite, and that this change in the carbonate phase had virtually no effect in the equilibrium chemistry of the solutions, but it did increase the solvent water masses for both GWB and ERDA-6. Adding a mixed Ca – Mg solid solution phase will be studied for possible inclusion in future databases.

In conclusion, the changes to the database and the addition of lead and iron reactants only elicited minor changes to the baseline solubilities, Am(III), Th(IV), and Np(V), pH, and TIC. It was necessary to reevaluate the calcite assumption and take the step of allowing calcite to precipitate to avoid an unrealistic disequilibrium in the carbonate system. The additional runs in this memo served to demonstrate that the baseline solubility model is robust regardless of the database and the calcite assumption, and that consistency has been maintained from CRA-2014 PA to the current CRA-2019 PA.

What Does the Future Hold?

Looking to the future, CRA-2019 PABC, may be necessary, and on to CRA-2024 PA and beyond, the baseline solubility model will continue to be developed in step with modifications to the Pitzer thermodynamic database, and any changes to the inventory. Updates to the database will include updating the actinide systems, the organics, borate, iron, potential addition of the sulfide system, and possibly adding a Ca – Mg carbonate solid solution phase.

REFERENCES

Brush, L.H., Y.-L. Xiong, J.W. Garner, A. Ismail, G.T Roselle, 2006. "Consumption of Carbon Dioxide by Precipitation of Carbonate Minerals Resulting from Dissolution of Sulfate Minerals in the Salado Formation In Response to Microbial Sulfate Reduction in the WIPP." Analysis report. Carlsbad, NM: Sandia National Laboratories. ERMS 544785.

Brush, L.H., and P.S. Domski. 2013. Prediction of Baseline Actinide Solubilities for the WIPP CRA-2014 PA. Carlsbad, NM: Sandia National Laboratories. ERMS 559138.

Domski, P.S. 2019. "Official Release of the Qualified Pitzer Thermodynamic Database, DATA0.FM4, for EQ3/6 under AP-183, Revision 1. Carlsbad, NM: Sandia National Laboratories. ERMS pending.

Domski, P.S. 2019. "Uncertainty Analysis of Actinide Solubilities for CRA 2019". Carlsbad, NM: Sandia National Laboratories. ERMS pending.

Domski, P.S. and C. Sisk-Scott. 2019. "Prediction of Baseline Actinide Solubilities for CRA 2019 with an Updated EQ3/6 Pitzer Thermodynamic Database, DATA0.FM4". Carlsbad, NM: Sandia National Laboratories. ERMS pending.

Sisk-Scott, C. 2019. "Calculation of Organic-Ligand Concentrations for the WIPP CRA-2019 Deferred PA" Carlsbad, NM: Sandia National Laboratories. ERMS 571011.

Wolery, T.J., and R.L. Jarek. 2003. "Software User's Manual: EQ3/6, Version 8.0." Software Document No. 10813-UM-8.0-00. Albuquerque, NM: Sandia National Laboratories.

Distribution:

SNL/WIPP Records Center (to be included in the AP-153 records package)